Supplement of

Steady-State Mixing State of Black Carbon Aerosols from a Particle-Resolved Model

Zhouyang Zhang et al.

Correspondence to: Jiandong Wang (jiandong.wang@nuist.edu.cn)

1 The simulation cases

1.1 Setup and result of the baseline case

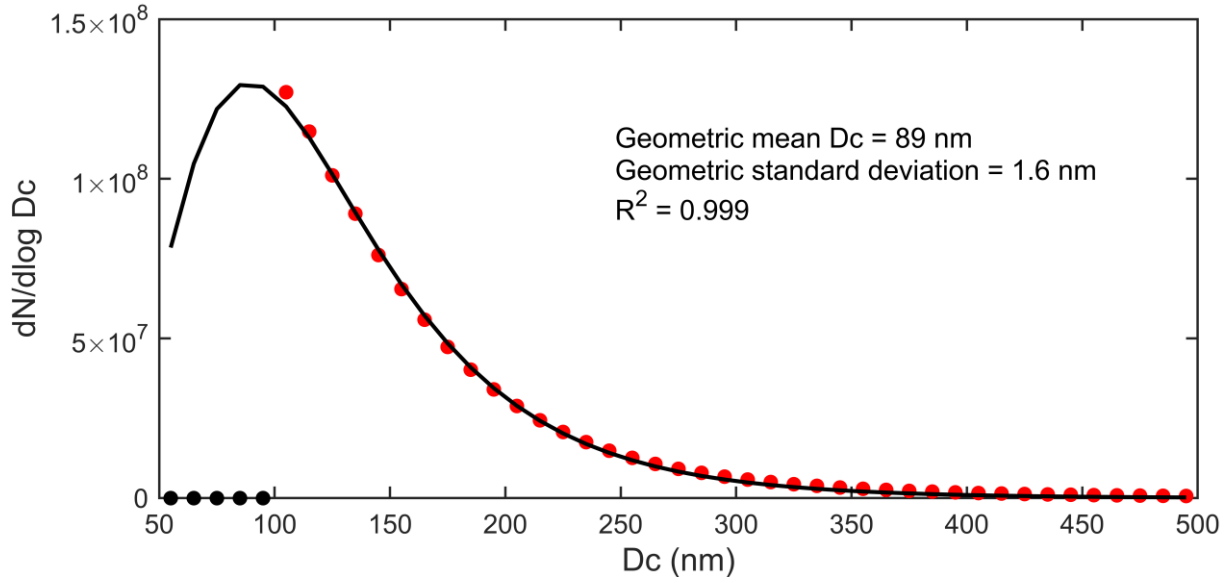

Figure S1. The distribution of the diameter of BC-core measured by single particle soot photometers (SP2) in the field observation in Nanjing. The red dots represent the statistical results, and the black line represents the fitting result. The fitting equation is: $\frac{N}{\sqrt{2\pi}\log\sigma}\exp(\frac{(\log Dc-\log\mu)^2}{2(\log\sigma)^2})$.

The distribution of the diameter of BC-core (Fig. S1) is the reference of BC emissions in Table S1.

Table S1. Input variables assigned in the baseline case

Environmental variable	**Value**
Temperature [K]	289
Relative humidity	0
Boundary layer height [m]	293.14
Mass loss (deposition)	constant
Latitude	0 °N
Day of year	July 19
Aerosol characteristic	**Value**
Emission rate [m^{-2} s^{-1}]	1.8×10^7
Fraction Bare-BC emissions	24.6%
Fraction Mix-BC emissions	2.4%

Fraction BC-free emissions	72.7%
Aerosol type	**Geo. mean dia. [nm]**
Bare-BC	89
Mix-BC	109
BC-free	110
Aerosol type	**Geo. standard dev.**
Bare-BC	1.60
Mix-BC	1.60
BC-free	1.70
Aerosol type	**Mass composition**
Bare-BC	100% BC
Mix-BC	68.3% BC, 31.7% OC
BC-free	100% OC
Emitted gas species	**Rate [mol · m^{-2} · s^{-1}]** with a total multiplication factor of 25 %
Sulfur dioxide	2.51×10^{-8}
Nitrogen dioxide	1.20×10^{-9}
Nitric oxide	2.50×10^{-8}
Ammonia	6.11×10^{-9}
Carbon monoxide	2.91×10^{-7}
Acetaldehyde	6.80×10^{-10}
Formaldehyde	1.68×10^{-9}
Ethene	7.20×10^{-9}
Internal olefin carbons	2.42×10^{-9}
Terminal olefin carbons	2.42×10^{-9}
Toluene	4.04×10^{-9}
Xylene	2.41×10^{-9}
Acetone	1.23×10^{-9}
Paraffin carbon	9.60×10^{-8}
Isoprene	2.30×10^{-10}
Methanol	2.80×10^{-10}
Alcohols	3.45×10^{-9}

Table S2. Comparison between measurement results (Wang et al., 2017) of bulk aerosol component mass fractions in different cities of China and in the PartMC-MOSAIC simulation. Since there are no sulfate-containing particles emitted and the sulfate production by in-cloud chemistry is not included, the primary source of SO_4 is the conversion of SO_2 gas to particles. As a result, the proportion of SO_4 mass is relatively small, while NO_3 levels are relatively high.

Aerosol components	The mass fraction range in measurement	The mass fraction in the model
OM	15~51%	26.7%
BC	0~12%	5.5%
NO_3	0.4~18%	27.1%
SO_4	3~35%	24.2%
NH_4	1~11%	16.6%

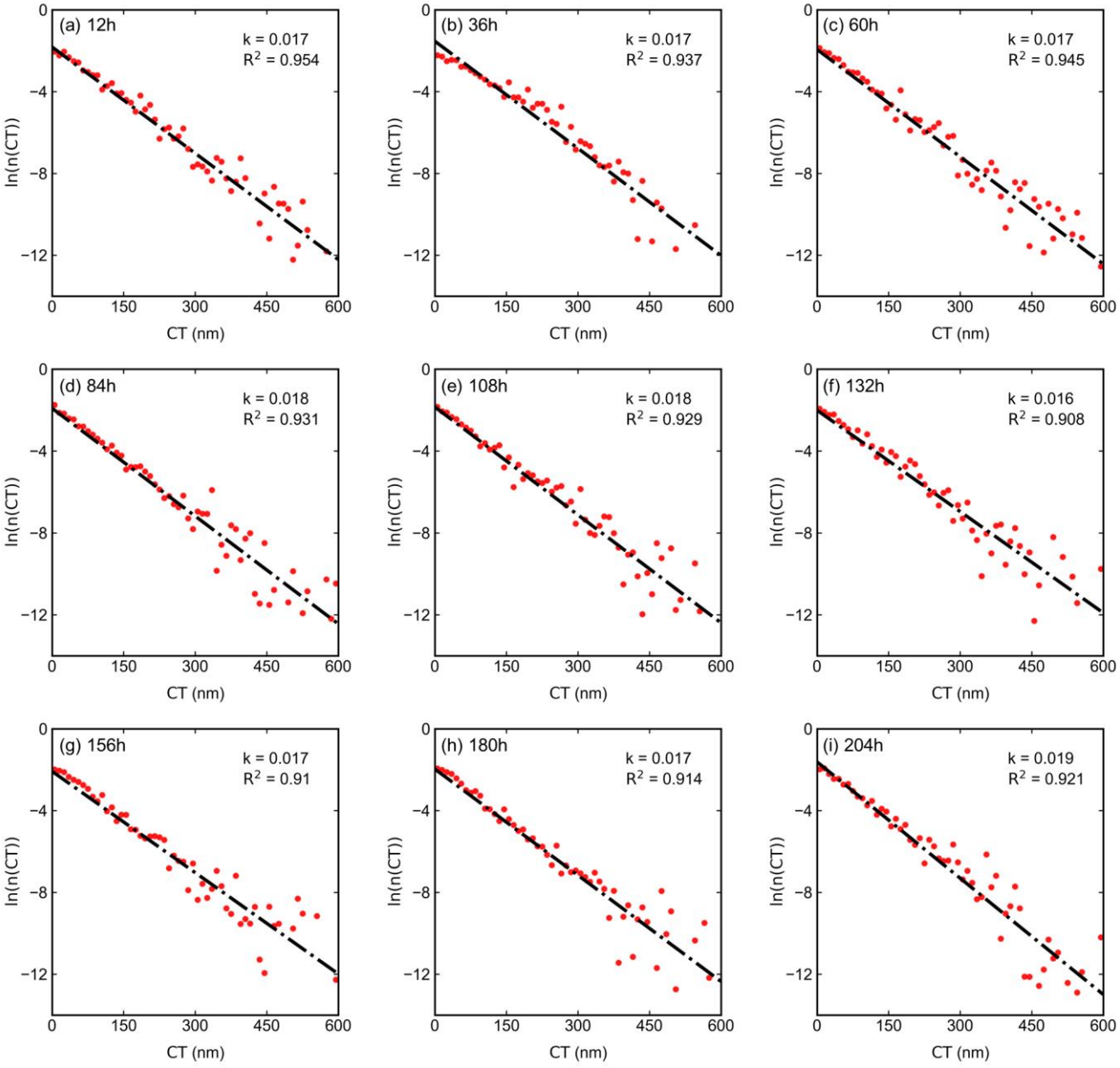

Figure S2. Coating thickness (CT) distribution of black carbon (BC) aerosols in the baseline case during simulation progress. Each subfigure shows the CT distribution for different simulation times (from 12 hours to 204 hours, with an interval of 24 hours). Under the combined influence of multiple atmospheric processes, the CT distribution rapidly exhibits an exponential linear distribution. As the simulation progresses, the BC mixing state remains steady (the overall correlation of linear fitting maintains a high value).

1.2 Setup and result of nine additional cases

The nine additional cases are created by altering pollution conditions (emission of aerosols and gas) and temperature conditions to confirm the universality of the steady mixing state of BC aerosols. Case 1: The temperature is 15 K higher than the temperature in the baseline case. Case 2: The temperature is 15 K lower than the temperature in the baseline case. Case 3: The geometric mean diameter of BC-core in particle emission is set to 70 nm (Bond et al., 2013), with a geometric standard deviation of 1.3 (Lee, 1983). Case 4: The geometric mean diameter of BC-core in particle emission is set to 200 nm (Moteki, 2023), with a geometric standard deviation of 1.3 (Lee, 1983). Case 5: The aerosol emission rate is increased to five times that of the baseline case. Case 6: The aerosol emission rate is reduced to one-fifth of that in the baseline case. Case 7: The gas emission rate is increased to five times that of the baseline case. Case 8: The gas emission rate is reduced to one-fifth of that in the baseline case. Case 9: The gas emissions are set to occur from 6:00 to 18:00 daily, with no emissions during the remaining hours.

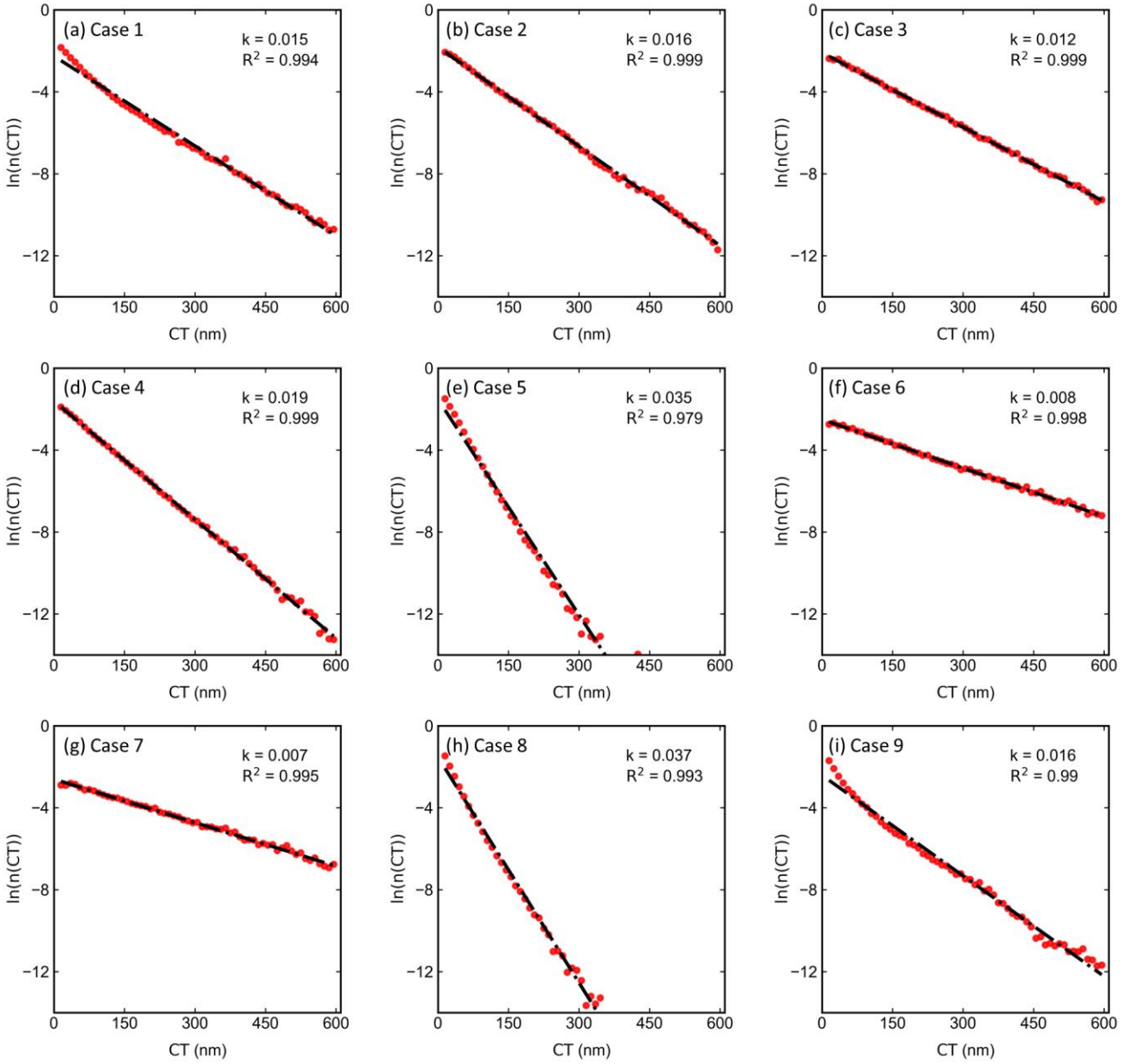

Figure S3. Results of CT distribution of BC aerosols in 9 simulation cases (excluding the Baseline case). The subfigures correspond to the results of cases 1 to 9. Each subfigure shows that the statistical CT distribution of BC aerosols follows the exponential linear distribution during the steady-state period (after 48 hours) simulated by PartMC-MOSAIC. The slope k = Dep/GR is determined by the deposition rate (Dep) and the growth rate (GR) (Wang et al., 2023). Temperature, aerosol and gas emissions can affect the GR, thereby indirectly affecting the k value. In the setup of the simulation cases, we fixed the deposition rate and altered temperature, emissions of particle and gas to change the growth rate. By comparing Case 1 (a) and Case 2 (b), we found that temperature has little effect on the k value (the higher the temperature, the smaller the k value); by comparing Case 3 (c) and Case 4 (d), we discovered that the larger median diameter of emitted BC-core brings a larger k value. Through the comparison of Case 5 to 8, we observed that a higher gas emission rate or a lower particle emission rate leads to a smaller k value (thicker coating).

Table S3. The characteristic time τ, equivalent CT (1/*k*), coefficient of determination of linear regression, and the average true CT value for ten different cases. The result shows that the characteristic time for black carbon (BC) aerosols approaching steady-state in a given region is influenced by the temperature, emissions rate of aerosols and gas, and the distribution of BC aerosols in emissions). In the baseline case and case 1 to 8, the value of equivalent CT is highly consistent with the value of average true CT. In the case 9, there is a certain discrepancy between the values of equivalent CT and average true CT (Fig. S3(i)). The deviation primarily arises from the data for which CT < 50 nm, where the thin coating layer is a result of intermittent emissions.

Scenario	Characteristic time (hour)	Equivalent CT (nm)	Coefficient of determination	Average true CT (nm)
Baseline case	3.2	62	0.999	63
Case 1	9.7	68	0.994	52
Case 2	2.4	62	0.999	63
Case 3	3.3	82	0.999	84
Case 4	3.1	52	0.999	54
Case 5	2.7	28	0.979	25
Case 6	3.6	127	0.998	124
Case 7	2.1	141	0.995	138
Case 8	7.1	27	0.993	21
Case 9	1.9	61	0.990	38

2 The data-process of PartMC-MOSAIC output

2.1 The slope *k* of the BC coating thickness distribution

The parameter *k* is determined by the distribution of BC coating thickness (CT = D_p - D_c) We first binned BC particles with respect to CT. The CT range of 0-600 nm (without the BC of CT = 0 nm) was divided into 60 bins with a bin width of 10 nm, corresponding to 60 data points. CT means the median CT of the corresponding bin, and ΔCT means the interval, which is set to 10 nm. Therefore, *n*(CT) means the number concentration of BC in the bin with the CT range of (CT-ΔCT/2, CT+ΔCT/2]. Next, we normalized the number concentration *n*(CT) of each particle size bin by dividing it by the total number concentration in the 0–600 nm segment. Then, we took the exponential transformations of each *n*(CT), resulting in multiple sets of corresponding ln(*n*(CT)) and CT data points (*n*(CT) is a dimensionless value because it is normalized). Finally, we make the linear regression analysis utilizing the least squares method to obtain slope *k* of the CT distribution. It is worth mentioning that in cases with smaller average CT, due to the precision limitations of PartMC, the data volume representing large CT ('n_part' in PartMC) is scarce, leading to noisybad simulation results. Therefore, we uniformly screen data points with ln(*n*(CT)) ≥ −14 (for all cases).

2.2 Diameters of BC-containing particle and BC-core

The particle size information of BC aerosols cannot be directly obtained from the simulation results of the PartMC-MOSAIC but requires postprocessing. Its calculation requires the combination of the assumption of a core-shell model (R. McGrory et al., 2022; Wang et al., 2019) and the densities of each component (Table S4). Before presenting the calculation method, we first make three initial assumptions: 1) BC-containing particles are spherical particles; 2) the BC component is concentrated at the center of the particle, also in the form of a regular sphere; 3) other components are uniformly mixed and coated on the surface of the BC-core. The mass composition of a BC particle can be represented as $\vec{\mu} = (\mu^1, \mu^2, ..., \mu^A)$, where a represents the number of components ranging from 1 to A. The diameter of the BC-core (D_c) is given by the following equation:

$$D_c = \sqrt[3]{\frac{6\mu^{BC}}{\pi\rho_{BC}}} \quad (1)$$

where ρ_{BC} represents the density of the BC component. The diameter of the particle (D_p) is determined by the equation below:

$$D_p = \sqrt[3]{\frac{6\mu_{all} - \pi {D_c}^3(\rho_{BC} - \rho_{other})}{\pi\rho_{other}}} \quad (2)$$

where ρ_{other} represents the weighted average density after uniform mixing of other components, which is given by the following equation:

$$\rho_{other} = \sum_{a=1,\, a \neq BC_{index}}^{A} \omega_a \cdot \rho_a \quad (3)$$

where ω_a denotes the proportion of component a within the mass composition of the particle coating layer, and the symbol ρ_a denotes the density of component a (Table S4).

Table S4. The densities of aerosol species used to calculate the mean density per particle.

Aerosol species	Density (kg/m^3)
SO_4	1800
NO_3	1800
Cl	2200
NH_4	1800
MSA	1800
ARO1	1400
ARO2	1400
ALK1	1400
OLE1	1400
API1	1400

API2	1400
LIM1	1400
LIM2	1400
CO_3	2600
Na	2200
Ca	2600
OIN	2600
OC	1000
BC	1800
H_2O	1000

2.3 Application of the moving average algorithm

The moving average algorithm is applied to eliminate the influence of regular external factors on the BC mixing state. Moving average (MA) is a simple and effective technique used to smooth time series data or remove noise from a dataset (Hansun, 2013). The algorithm employed in this study calculates the mean value of data points within a designated time window or interval. As new data points emerge, the window shifts or progresses along the time series, thereby generating a continuous curve that accentuates the fundamental trend or pattern in the data while mitigating the influence of stochastic fluctuations. To address the dynamic changes in the BC mixing state, we employ the simple moving average (SMA) algorithm to minimize the impact of diurnal variations. The window size is set to 24 hours in this paper, and the data points within the window are summed and divided by the window size to obtain the processed value. For instance, the value recorded at 12:00 represents the mean value of the preceding 1 to 24 hour period, while the value at 13:00 corresponds to the average value of the 2 to 25 hour period. Consequently, upon implementing the moving average technique, the temporal span of the data shifts from 240 (1 to 240) hours to 217 (12 to 228) hours. The smoothing effect of SMA processing on the BC mixing state in a 10-day simulation mitigates daily fluctuations, thereby enabling a more comprehensive analysis of the overall changes in mixed states.

References

Bond, T. C., Doherty, S. J., Fahey, D. W., Forster, P. M., Berntsen, T., DeAngelo, B. J., Flanner, M. G., Ghan, S., Kärcher, B., Koch, D., Kinne, S., Kondo, Y., Quinn, P. K., Sarofim, M. C., Schultz, M. G., Schulz, M., Venkataraman, C., Zhang, H., Zhang, S., Bellouin, N., Guttikunda, S. K., Hopke, P. K., Jacobson, M. Z., Kaiser, J. W., Klimont, Z., Lohmann, U., Schwarz,

J. P., Shindell, D., Storelvmo, T., Warren, S. G., and Zender, C. S.: Bounding the role of black carbon in the climate system: A scientific assessment, J. Geophys. Res. Atmospheres, 118, 5380–5552, https://doi.org/10.1002/jgrd.50171, 2013.

Hansun, S.: A new approach of moving average method in time series analysis, in: 2013 Conference on New Media Studies (CoNMedia), 2013 Conference on New Media Studies (CoNMedia), 1–4, https://doi.org/10.1109/CoNMedia.2013.6708545, 2013.

Lee, K. W.: Change of particle size distribution during Brownian coagulation, J. Colloid Interface Sci., 92, 315–325, https://doi.org/10.1016/0021-9797(83)90153-4, 1983.

Moteki, N.: Climate-relevant properties of black carbon aerosols revealed by in situ measurements: a review, Prog. Earth Planet. Sci., 10, 12, https://doi.org/10.1186/s40645-023-00544-4, 2023.

R. McGrory, M., H. Shepherd, R., D. King, M., Davidson, N., D. Pope, F., Matthew Watson, I., G. Grainger, R., C. Jones, A., and D. Ward, A.: Mie scattering from optically levitated mixed sulfuric acid–silica core–shell aerosols: observation of core–shell morphology for atmospheric science, Phys. Chem. Chem. Phys., 24, 5813–5822, https://doi.org/10.1039/D1CP04068E, 2022.

Wang, A., Chan Miller, C., and Szostak, J. W.: Core-Shell Modeling of Light Scattering by Vesicles: Effect of Size, Contents, and Lamellarity, Biophys. J., 116, 659–669, https://doi.org/10.1016/j.bpj.2019.01.006, 2019.

Wang, J., Zhao, B., Wang, S., Yang, F., Xing, J., Morawska, L., Ding, A., Kulmala, M., Kerminen, V.-M., Kujansuu, J., Wang, Z., Ding, D., Zhang, X., Wang, H., Tian, M., Petäjä, T., Jiang, J., and Hao, J.: Particulate matter pollution over China and the effects of control policies, Sci. Total Environ., 584–585, 426–447, https://doi.org/10.1016/j.scitotenv.2017.01.027, 2017.

Wang, J., Wang, J., Cai, R., Liu, C., Jiang, J., Nie, W., Wang, J., Moteki, N., Zaveri, R. A., Huang, X., Ma, N., Chen, G., Wang, Z., Jin, Y., Cai, J., Zhang, Y., Chi, X., Holanda, B. A., Xing, J., Liu, T., Qi, X., Wang, Q., Pöhlker, C., Su, H., Cheng, Y., Wang, S., Hao, J., Andreae, M. O., and Ding, A.: Unified theoretical framework for black carbon mixing state allows greater accuracy of climate effect estimation, Nat. Commun., 14, 2703, https://doi.org/10.1038/s41467-023-38330-x, 2023.